The New Zealand Reanalysis (NZRA): development and preliminary evaluation

Amir Pirooz[1], Stuart Moore[1], Trevor Carey-Smith[1], Richard Turner[1], Chun-Hsu Su[2]

[1] National Institute of Water and Atmospheric Research (NIWA), Wellington 6021, New Zealand
[2] Bureau of Meteorology, Docklands, Victoria 3008, Australia

ABSTRACT

The New Zealand Reanalysis (NZRA) is the first high-resolution convection-permitting atmospheric regional reanalysis model over Aotearoa New Zealand (NZ). NZRA has a spatial horizontal grid spacing of 1.5km and is forced using data from the Bureau of Meteorology Atmospheric high-resolution Regional Reanalysis for Australia (BARRA-R) with approximately 12km horizontal grid spacing. This paper outlines the development of NZRA, including the numerical weather forecast model and driving model. In addition, the performance of NZRA is compared against BARRA-R and global reanalysis products (ERA-Interim and ERA5) and validated against observational data collected during June-July 2014 as part of the Deep Propagating Gravity Wave Experiment (DEEPWAVE) field campaign. The results demonstrate that dynamically downscaling BARRA-R to NZRA considerably enhances the wind and temperature predictions, particularly capturing well the diurnal temperature cycle, wind speeds above 95th percentile, and gust wind speeds over the high elevation regions of NZ. In addition, NZRA provides better estimates of total precipitation over the North Island, Canterbury region, West Coast and the southern part of the South Island compared to the Virtual Climate Station Network (VCSN) gridded observation-based product, other reanalyses and NIWA's operational convective-scale forecast model, NZCSM, as was run in 2014.

1. INTRODUCTION

Atmospheric reanalyses provide physically coherent and long-term spatially complete records of various climate variables (Su et al., 2019; Minola et al., 2020) and are today among the most used datasets in climatological and geophysical research, due to the fact that they are able to generate consistent series of various climate variables (Dee et al., 2011). The key benefit is from being able to re-forecast historical periods using modern forecast models and data assimilation techniques, such as four-dimensional variational data assimilation (4D-Var) (Bannister, 2017), that make better use of observation data from various sources.

Although global-scale reanalyses have advanced significantly in quality and provide physically coherent and long-term spatially complete information for the whole globe, their spatial and temporal resolutions are still relatively coarse and it has been demonstrated that, with spatial resolutions typically greater than 30-50km, they may not be able to capture small-scale meteorological process and other sub-grid phenomena, particularly over complex terrain (Mesinger et al., 2006; Yoshimura and Kanamitsu, 2008; Su et al., 2019). The coarse resolution of global reanalyses has also implications on quality and impactfulness of subsequent studies, such as the hydrological response to climate change scenarios (Miller et al., 2003), wind speed over complex terrain (Minola et al., 2020), the impact of climate change on agriculture (Fuhrer et al., 2006), energy (Zhang et al., 2018; Frank et al., 2020), extreme winds (Steinheuer and Friederichs, 2020; Taszarek et al., 2020), and rainfall (Gleixner et al., 2020; Hu and Franzke, 2020).

Tetzner et al. (2019) conducted a regional evaluation of meteorological parameters in the southern Antarctic Peninsula and Ellsworth Land using two global reanalyses, namely ERA5 (Hersbach et al., 2020) and its predecessor ERA-Interim (Dee et al., 2011), from the European

Centre for Medium-Range Weather Forecasts (ECMWF). Although the higher resolution ERA5 outperformed ERA-Interim by reducing the cold coastal biases and had a better representation of near-surface air temperature and wind speed, both the reanalyses underestimated wind speed, which could be attributed to the effects of topographic features. Validating ERA5 and ERA-Interim against observations across Norway and Sweden, Minola et al. (2020) also showed that both reanalyses underestimate high wind speeds.

Dynamically downscaling global reanalyses to higher-resolution regional reanalyses could address the shortcomings of the global reanalysis datasets (Komurcu et al., 2018; Steinke, 2019; Su et al., 2019; Lu et al., 2021). Regional reanalyses can potentially provide more detailed meteorological information than global models, by leveraging recent advances in higher resolution regional numerical weather prediction (NWP) models and data assimilation systems (Frank et al., 2020; Lu et al., 2021). This is achieved by nesting a high-resolution NWP model within a global reanalysis (e.g., ERA5). Due to their higher spatial and temporal resolutions, these regional models can resolve small-scale forcing events, such as convection (Frank et al., 2020; Su et al., 2021), and represent extremes of variables more accurately (Komurcu et al., 2018; Steinheuer and Friederichs, 2020).

Comparison between 2 and 6km regional reanalyses against the ~80km resolution ERA-Interim, Steinke (2019) demonstrated that instantaneous, daily and monthly integrated water vapour are significantly better represented in the regional reanalyses. Due to their higher spatial and temporal resolutions, regional reanalyses can more accurately capture the timing, intensity, and spatial extent of climate and environmental variables (Leeper et al., 2017; Lu et al., 2019). For example, better representation of wind gust speeds in higher resolution regional reanalyses enabled Steinheuer and Friederichs (2020) to estimate the wind gust speeds at different vertical heights using 10-m gust wind outputs and other climate variables. The Indian Monsoon Data Assimilation and Analysis (IMDAA) dataset, a high-resolution reanalysis with 12km horizontal resolution, has been shown to outperform ERA-Interim over India (Ashrit et al., 2020). Acharya et al (2019) evaluated the performance of the Bureau of Meteorology Atmospheric high-resolution Regional Reanalysis for Australia (BARRA-R) (Su et al., 2019) in predicting spatio-temporal characteristics of precipitation fields across Australia. It was demonstrated that BARRA-R outperforms its driving model, ERA-Interim, and better represents the distribution of wet days and transition probabilities.

Frank et al. (2020) demonstrated that the recently developed convective-scale regional reanalysis system for Central Europe (COSMO-REA2) with a spatial horizontal resolution of 2km provides considerable improvement in predictions of wind field and precipitation on different time scales compared with coarser gridded global reanalyses. Having compared the performances of four global and three regional reanalyses in representing near-surface temperature and precipitation, Keller and Wahl (2021) showed that although regional reanalyses add value over global reanalyses, particularly for precipitation, the performance of reanalysis models varies considerably not only between the models, but also between variables and locations. Thus, the use of reanalyses strongly depends on the specific application and region. Safaei Pirooz et al. (2022) compared the performance of three global reanalyses and BARRA-R over New Zealand and concluded that BARRA-R generally outperforms the other reanalyses.

It is evident that high-resolution regional reanalyses significantly enhance the prediction of climate variables and their spatio-temporal variability. Gaining a better understanding of the past climate and the mechanisms leading to extremes and general climatology is essential for many environmental, engineering, and meteorological studies as well as for improving climate projection model estimates. Currently, the highest resolution regional reanalysis available for New Zealand is the BARRA-R model (Su et al., 2019), which utilises the UK Met Office Unified Model (UM) with a horizontal resolution of 12km and uses ERA-Interim as the driving model. Su et al. (2021) downscaled BARRA-R reanalysis to 1.5km horizontal resolution, called BARRA-C, over four major Australian cities. It was demonstrated that BARRA-C provides additional skill over BARRA-R, with wind and temperature performance, particularly over complex and coastal regions, enhanced compared with the 12km BARRA-R model. Improvements were also observed in BARRA-C predictions of the timing and intensity of precipitation during convective events as well as in the spatial distribution of sub-daily rainfall totals.

In this study, we describe the development of the New Zealand Reanalysis (NZRA) whereby BARRA-R is dynamically downscaled to a 1.5km horizontal grid spacing over New Zealand. NZRA uses the UM and after completion will cover the 1990-2018 period. The aim of our research is to demonstrate the added value of the NZRA over its

driving model (BARRA-R) and global reanalyses (ERA5 and ERA-Interim). The paper is structured as follows. In Section 2, we outline the NZRA setup and configuration as well as the other datasets used in the paper. The evaluation of NZRA over a trial period of June-July 2014 against point-based observations and an observation-based interpolated gridded dataset is presented in Section 3, focusing on precipitation, air temperature, mean and gust wind speeds. Lastly, Section 4 summarises our findings and discusses the added skills of NZRA over other reanalyses.

2. METHODOLOGY AND DATA

2.1 NZRA

The first high-resolution convection-permitting regional reanalysis model for New Zealand, the New Zealand Reanalysis (NZRA), has been developed at the National Institute for Water and Atmospheric Research (NIWA) and is based on the UK Met Office Unified Model (UM) (Davies et al., 2005). The UM is a non-hydrostatic, fully compressible, deep-atmosphere model whose dynamical core, ENDGame (Even Newer Dynamics for General atmospheric modelling of the environment), solves the equations of motion using mass-conservation, semi-implicit, semi-Lagrangian, time-integration methods (Wood et al., 2014). A comprehensive description of parameterisations and physics schemes included in UM can be found in Bush et al (2020).

The NZRA domain (Figure 1a) is the same as NIWA's operational convective-scale forecast model. The NZRA model has a horizontal grid spacing of 0.0135° × 0.0135° (approximately 1.5km) on a rotated pole coordinate system, comprising 1350 × 1200 grid points in the north-south (meridional) and west-east (zonal) directions respectively. The NZRA domain has 70 vertical levels extending from near the surface to 40km above sea level. Near the surface, vertical levels follow the modelled orography and then relax to a uniform radial height above about 18km (62 model levels). The model is run with an integration timestep of 60s. Figure 1b depicts the NZRA's model orography as well as the location of the point observations used in this study at Hokitika.

The development of NZRA is similar to NIWA's operational New Zealand Convective-Scale Model (NZCSM) but features some differences in the science configuration, driving model and forecast length. NZRA uses the same ancillary input data as NZCSM, including orography, land-sea mask, canopy heights and other land cover data. The model uses an underlying orography created at the model resolution of 1.5km from the 1 km horizontal resolution Global Land One-km Base Elevation (GLOBE) dataset (GLOBE Task Team, 1999). Land cover data are based on the Climate Change Initiative (CCI) (Hartley et al., 2017).

NZRA is a downscale-only system that takes its initial and lateral boundary conditions from BARRA-R (Su et al.,

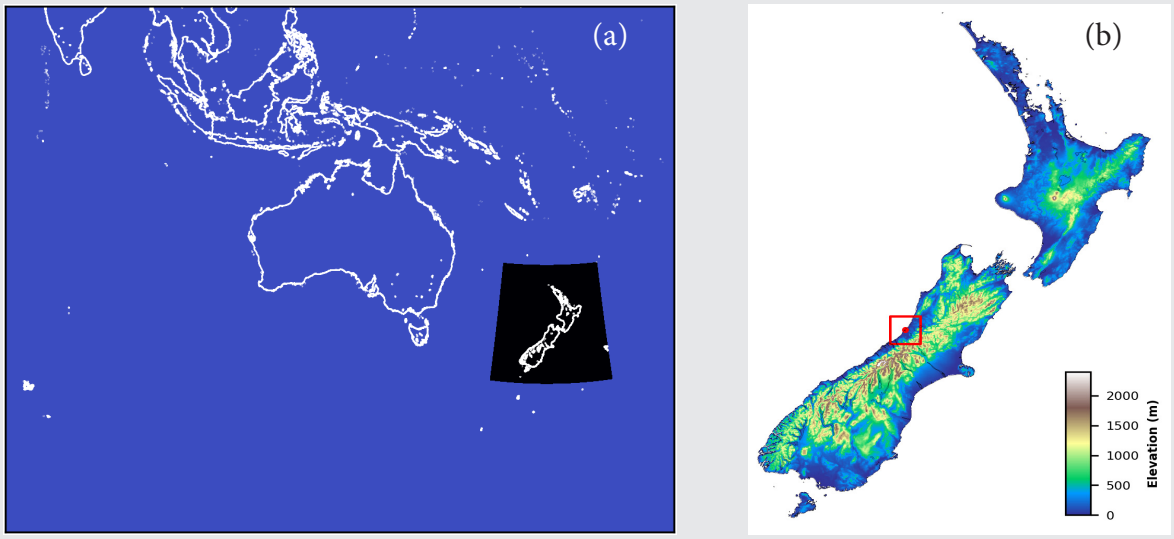

Figure 1: (a) BARRA-R 12km reanalysis (blue) and NZRA/NZCSM (black) domains. (b) NZRA model orography and the location of point observations used in this paper.

	Name	Reference	Spatial Resolution	Temporal Resolution	Model Cycle
Global	ERA-Interim	Dee et al. (2011)	80km	3-hourly	Cy31r2 (2006)
	ERA5	Hersbach et al. (2020)	31km	Hourly	Cy41r2 (2016)
Regional	BARRA-R	Su et al. (2019)	12km	Hourly	UM 10.2
	NZCSM (as run in 2014)	Carey-Smith and Andrews (2016) Turner and Moore (2017)	1.5km	30 mins	UM 8.4
	NZRA	Current paper	1.5km	30 mins	UM 11.4

Table 1: Global- and regional-scale reanalysis datasets used in this study.

2019). The NZRA model is re-initialised every six hours on the synoptic hours, 00:00, 06:00, 12:00 and 18:00 UTC. Lateral boundary conditions have a 30-minute temporal resolution. This setup allows for the development of larger-scale features within NZRA. Similar to BARRA-C (Su et al., 2021), each hindcast in NZRA is a nine-hour simulation, however, the first three hours are discarded due to model spin-up and only the last six hours saved. During the spin-up period the interior of the higher resolution model domain is establishing the finer atmospheric motions that may only partially be present in the coarser resolution initial conditions and we choose to ignore this period to ensure the continuous NZRA dataset is minimally impacted by this adjustment process.

The science configuration used in NZRA is the midlatitude version of the second Regional Atmosphere and Land configuration (RAL2–M) (Bush et al., 2020). Unlike its driving model BARRA-R, NZRA does not use a convection parametrisation scheme. Therefore, NZRA relies on the model dynamics to represent convective motion. As outlined in Su et al (2021), although at 1.5km resolution convection and other small-scale processes are not fully resolved, it is known that removal of the cumulus parametrisation provides more realistic behaviour (Clark et al., 2016) and an overrepresentation of low rainfall rates can be improved via the introduction of the Leonard term into the UM's sub-grid mixing scheme as described in Hanley et al (2019) and implemented in the RAL2-M science configuration used by NZRA.

2.2. Other Reanalysis and Point-Observation Data

For point-based assessment, observation data collected at Hokitika, New Zealand, during June-July 2014 as part of the Deep Propagating Gravity Wave Experiment (DEEPWAVE)[1] campaign over New Zealand (Fritts et al., 2016) were used. Considering that data from most meteorological stations across New Zealand have been incorporated into the BARRA-R's data assimilation system, the DEEPWAVE data provides a set of independent observations that can be used for this preliminary assessment of the NZRA.

DEEPWAVE studied the dynamics of gravity waves (GWs) from the surface of the Earth to the mesosphere and lower thermosphere. The project examined how tropospheric winds and storms modulate the generation of GWs. The project also examined how GWs propagate across the tropopause into the stratosphere including the polar night jet and tidal winds that influence GW propagation and breakdown in the middle atmosphere. The data collected during this period have been used for various scientific objectives, including investigation of orographically induced GW (Witschas et al., 2017), GW propagation (Ehard et al., 2016; Fritts et al., 2016), and moist biases in various configuration of the UM (Yang et al., 2017).

Here, high-temporal resolution (30-sec) point-based observation data of rain rate, surface temperature and wind speed are used to evaluate the NZRA performance for this trial period. The observed temporal resolution was down-sampled to match the reanalysis outputs, e.g., 30-min instantaneous winds and temperature and 30-min accumulated rainfall.

In addition to these observation data, two global reanalyses, ERA-Interim and ERA5, one regional reanalysis, BARRA-R, and one operational forecast model, NZCSM, were also compared against NZRA. Table 1 summarises the

[1] https://www.eol.ucar.edu/field_projects/deepwave

main specifications of the NWP models used in this study. It should be noted that for the verification period used in this study (June-July 2014), an older version of UM employing the New Dynamics dynamical core, was in use by the NZCSM. The ENDGame dynamical core used in current versions of the UM was introduced in the NZCSM in 2017. Therefore, the results of NZCSM in this study should not be interpreted as the current performance of NZCSM.

To spatially compare precipitation, a gridded precipitation dataset based on interpolated observation data, called the Augmented Virtual Climate Station Network (VCSN), is used. The Augmented VCSN, which contains daily precipitation data at 5km grid resolution, incorporates considerably more rain observations (around 1200) compared to the original version of the VCSN (Tait and Turner, 2005; Tait et al., 2006; Tait et al., 2012).

3. RESULTS AND DISCUSSION

3.1 Point-Based Observation at Hokitika

3.1.1 Wind speed

Figure 2 shows percentile (or Q-Q) plots comparing the reanalyses and observation 10m wind speed deviations from mean values. The percentile plots provide an indication of how the reanalysis resolves the extremes. In addition, differences between observed and reanalysed wind speed at several percentiles are tabulated in Table 2. As illustrated in Figure 2 and Table 2, NZRA more closely matches the observed wind speed even at higher percentile thresholds in comparison to other reanalysis products. In particular, the NZRA wind speed is closer to that of the observations above the 90th percentile and up to the 99.5th percentile, while the other reanalyses, particularly ERA-Interim and

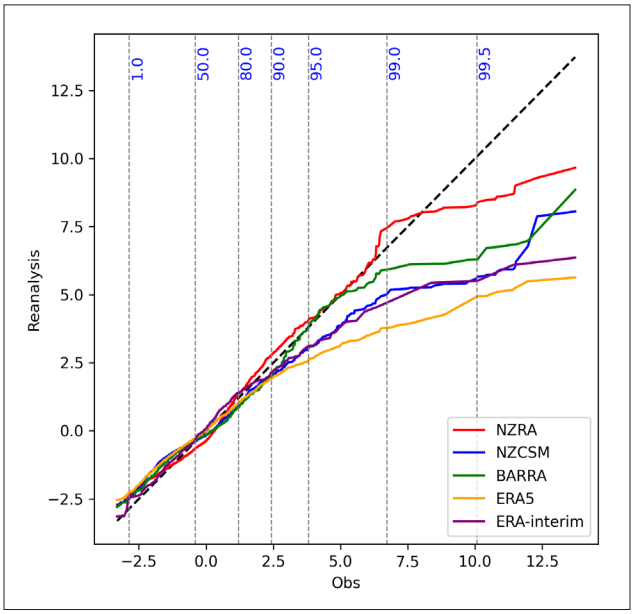

Figure 2: Comparisons of percentile values between observations at Hokitika and reanalyses for 10m wind speed. The vertical dash lines indicate the corresponding percentiles of the observations.

ERA5, strongly underestimate the wind speed. In addition, NZRA outperforms and adds significant value over its driving model, BARRA-R, in estimating strong winds. The underestimation of strong winds in reanalyses could be attributed to many potential reasons, such as the model's representation of orography, land cover data including vegetation types and roughness, poor modelling of wind speeds in unstable conditions, and gust parameterisation as elaborated on in (Rose and Apt, 2016; Su et al., 2019; Minola et al., 2020).

Correlation (R^2) values and slope (S) of the best fit line between reanalyses and observations for 10m wind speed are illustrated in Figure 3. Overall, NZRA has higher R^2 and S values against observations than the other datasets. Figure 4 compares the timeseries of wind speed from the

	10m wind speed (ms^{-1})				
Percentiles >	**1**	**90**	**95**	**99**	**99.5**
NZRA	0.458	0.348	0.240	0.732	–1.694
NZCSM	0.423	–0.423	–0.784	–1.707	–4.432
BARRA-R	0.362	–0.388	–0.004	–0.772	–3.798
ERA5	0.597	–0.518	–1.193	–2.922	–5.152
ERA-int	0.337	–0.297	–0.694	–1.944	–4.588

Table 2: Difference ($m\ s^{-1}$) between observed and reanalyses wind speeds at various percentiles.

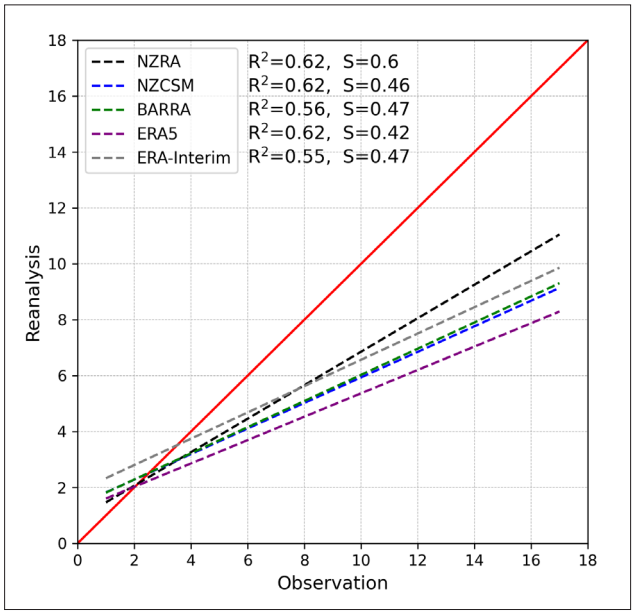

Figure 3 (above): Linear relationship between reanalysis and observed 10m wind speed. "S" and "R^2" are the slope and correlation of the best fit line, respectively.

reanalyses and point observation at the Hokitika location. NZRA predicts peak wind speeds and sudden increases/decreases in wind speed magnitudes more accurately compared to the other products.

3.1.2. Surface temperature

Similar to Figure 2, Figure 5 depicts percentile (or Q-Q) plots of 2m surface temperature from the reanalyses and observations and Table 3 shows the differences between these values at various percentiles. The NZCSM (as was run in 2014) and ERA5 overestimate and underestimate surface temperature in regimes below the 25th percentile and above the 50th percentile respectively. Although ERA-Interim also overestimates the low percentile temperatures, it provides better estimates of high percentile temperatures

Figure 4 (below): Comparison of 10m wind speed timeseries between each reanalysis dataset and observations at Hokitika. Time is in UTC.

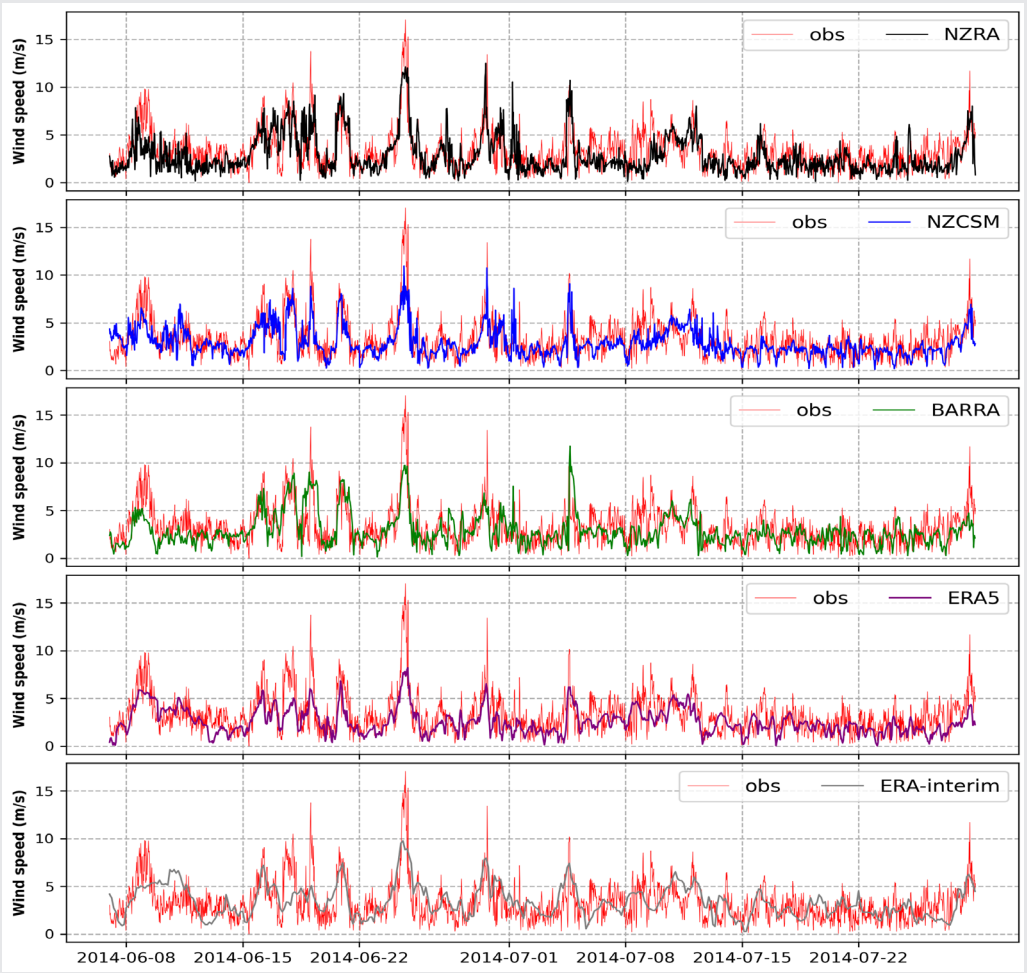

than that of ERA5 and NZCSM. NZRA and BARRA-R temperature show the best agreement with the observations for all percentiles, with NZRA marginally outperforming BARRA-R when compared across all percentiles. NZRA does tend to overestimate surface temperatures at the higher percentile range, while other datasets underestimate.

The average differences between the reanalysis datasets and the observed surface temperature, presented as a diurnal cycle during June-July 2014 are shown in Figure 6. ERA-Interim demonstrates a significant cold bias, considerably underestimating the temperature at all hours. Unlike other products, NZCSM shows a warm bias of about +1°C between 06:00 to 21:00 UTC. NZRA, BARRA-R and ERA5 have a similar bias and all depict a cold bias at all hours. NZRA does however have a smaller bias from 06:00 to 14:00 UTC compared to BARRA-R.

Figure 7 compares the timeseries of surface temperature from the reanalyses and point observations at the Hokitika location. NZRA performs considerably better than the ERA datasets and NZCSM, and marginally better than

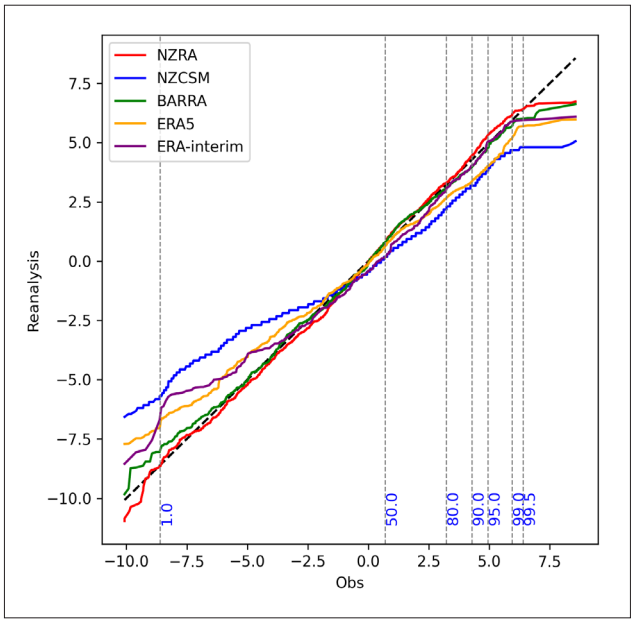

Figure 5: Comparisons of percentile values between observations at Hokitika and the reanalyses for 2m surface temperature. The vertical dash lines indicate the corresponding percentiles of the observations.

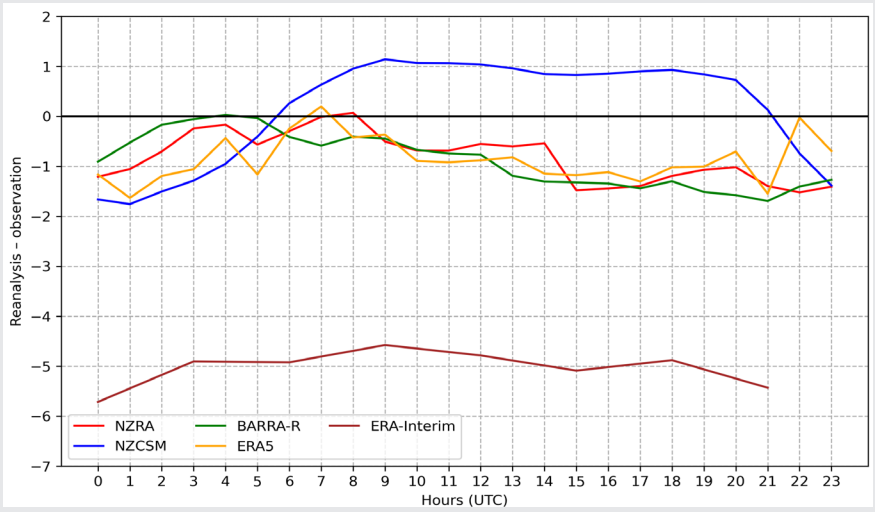

Figure 6: Hokitika diurnal surface temperature average difference between the reanalyses and observations.

	2m surface temperature				
Percentiles >	**1**	**90**	**95**	**99**	**99.5**
NZRA	–0.037	0.160	0.356	0.236	0.005
NZCSM	2.931	–1.106	–1.129	–1.264	–1.620
BARRA-R	0.577	–0.320	–0.154	–0.212	–0.411
ERA5	1.574	–0.929	–0.925	–0.727	–0.734
ERA-int	1.929	–0.247	0.086	–0.063	–0.481

Table 3: Difference between observed and reanalysed surface temperature at various percentiles.

BARRA-R in capturing high and low temperatures as well as daily cycles (see 2014-07-15 to 2014-07-31 UTC). Linear relationships along with correlation values (R^2) and slopes (S) of the best fit line between reanalyses and observations are illustrated in Figure 8. Overall, NZRA has higher R^2 and S values against observations than the other datasets.

To further investigate the performance of the reanalyses' predictions of extreme temperatures, Table 4 summarises the statistical scores, including Pearson's correlation, root-mean squared error (RMSE), bias and mean absolute error (MAE), for daily minimum and maximum surface temperature against the point observations.

Table 4 indicates that for daily maximum surface temperature, NZRA has the best scores among all the considered reanalyses, except for the correlation value where NZCSM and ERA5 have slightly higher values than NZRA. NZRA has the smallest MAE in daily minimum temperature. However, ERA5 shows smaller bias and

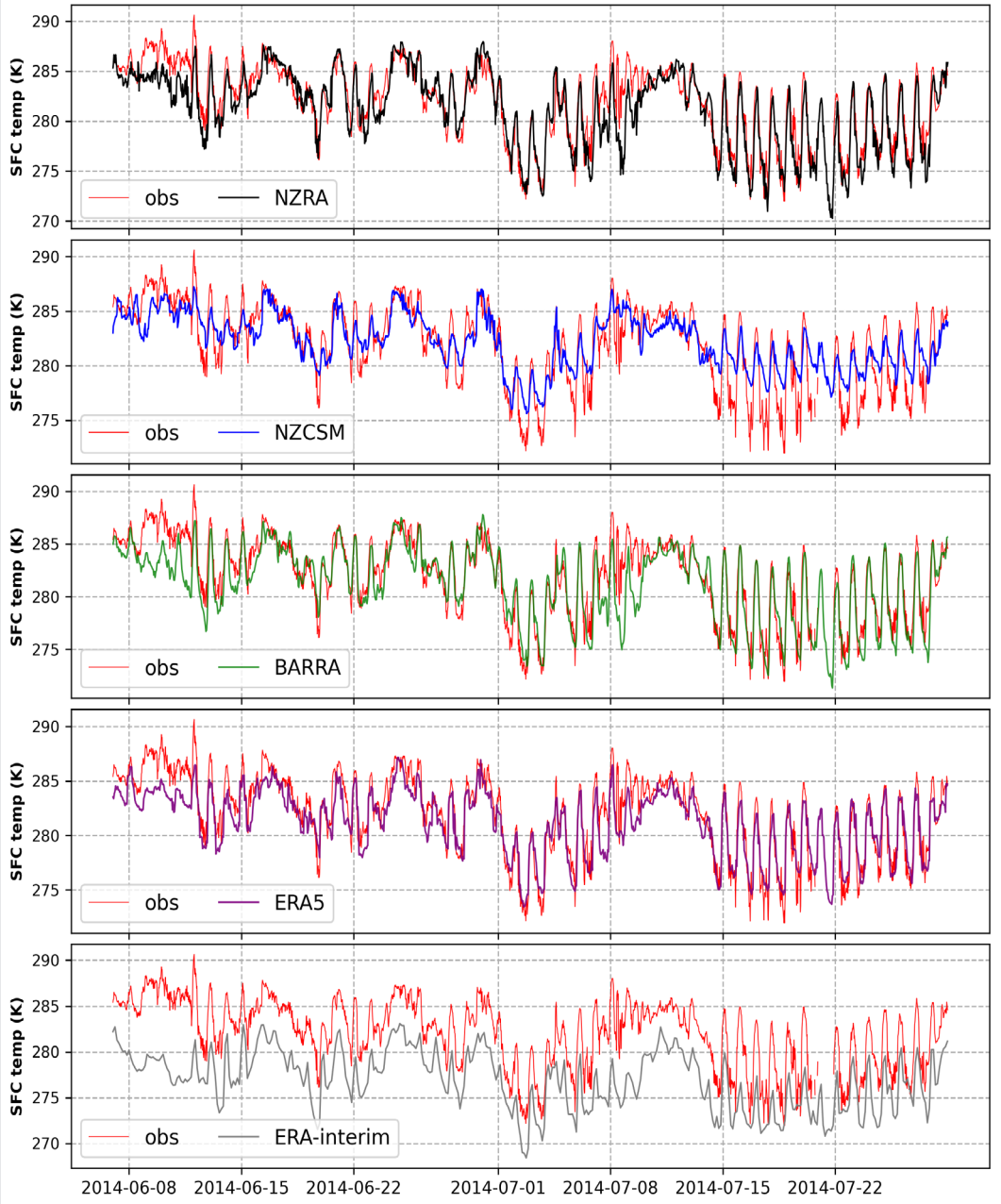

Figure 7: Comparisons of surface temperature timeseries between reanalyses and observation. Time is in UTC.

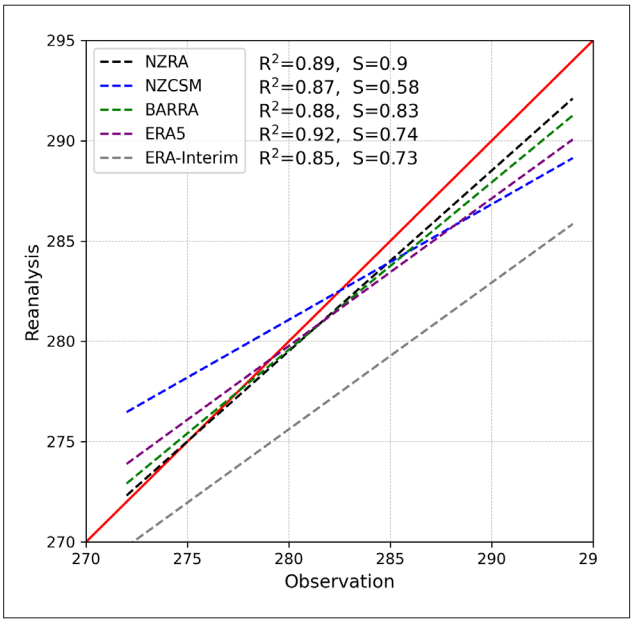

Figure 8: Linear relationship between reanalysis and observed 2m surface temperature. "S" and "R^2" are the slope and correlation of the best fit line, respectively.

simulated by NZRA and NZCSM and measured at Hokitika during June-July 2014 are compared in Figure 9a. NZRA appears to capture a larger proportion of the higher rainfall rates more accurately than NZCSM does, although errors in timing and intensity do remain. For closer inspection, the daily accumulated rainfall amounts from NZRA, NZCSM and also BARRA-R are shown in Figure 9b and compared with observed values. It appears that all three products provide reasonably accurate estimates of daily precipitation amount on the daily timescale, though all datasets both under- and over-predict the daily amounts, sometimes considerably so, over the course of the DEEPWAVE campaign period. The statistical scores comparing observations with the NZRA, NZCSM and BARRA-R datasets for daily precipitation are shown in Table 5. The scores from all the considered models are relatively similar, however NZRA whilst having the lowest MAE (good) does exhibit the worst correlation, RMSE and bias values.

Figure 10 depicts the percentile comparison plot of

	Daily minimum temperature				Daily maximum temperature			
	Corr.	**RMSE**	**Bias**	**MAE**	**Corr.**	**RMSE**	**Bias**	**MAE**
NZRA	0.926	1.718	–0.702	1.213	0.816	1.247	–0.425	0.883
NZCSM	0.863	2.909	1.684	2.318	0.912	1.488	–1.228	1.296
BARRA-R	0.904	1.763	–0.375	1.317	0.796	1.326	–0.488	0.913
ERA5	0.946	1.534	0.163	1.230	0.868	1.578	–1.201	1.275
ERA-Int	0.898	4.124	–3.691	3.719	0.601	5.890	–5.606	5.606

Table 4: Statistical scores for daily minimum and maximum surface temperature between observations and reanalyses.

RMSE and higher correlation values. BARRA-R, although performing worse than NZRA generally, has slightly smaller bias value compared with NZRA for daily minimum temperature.

3.1.3. Precipitation

Safaei Pirooz et al. (2022) demonstrated that ERA5 and ERA-Interim perform poorly in their predictions of precipitation compared with higher resolution products such as BARRA-R, particularly over the mountainous regions and west coast of the South Island. Therefore, in this section, only the precipitation estimates of NZCSM, NZRA and BARRA-R are compared against observations. Instantaneous rainfall rates at 30 minute intervals as NZRA, NZCSM and BARRA-R hourly precipitation amounts greater than 1mm. Similar performance is found across all the datasets at the lowest percentiles ranges (up to 50th percentile) after which all begin to noticeably underpredict precipitations compared to the observations. NZCSM performs better than NZRA and BARRA-R at the more extreme percentile range, explaining the results in Table 5. Considering the short timeseries used in this verification and that this is just one location, not representative of all of NZ, in future, a more comprehensive assessment of NZRA rainfall will be conducted.

3.2. Spatial comparison

This section presents an evaluation of spatial variability

	Corr.	RMSE	Bias	MAE
NZRA	0.849	9.012	-2.584	3.910
NZCSM	0.850	7.753	-0.190	4.348
BARRA-R	0.862	7.787	-1.892	4.078

Table 5: Statistical scores for daily accumulated precipitation between observation and reanalyses.

$$\%bias = 100 \times \frac{mean(d_m) - mean(d_0)}{mean(d_0)}$$

Equation 1: Where d_m and d_0 are the daily accumulated precipitations from the reanalyses and VCSN, respectively.

In addition, MAE values of total precipitation during 30/05/2014 – 01/08/2014 averaged over the North and South Islands are summarised in Table 6. It is evident that NZRA shows smaller MAE over both islands compared with NZCSM and its driving model BARRA-R.

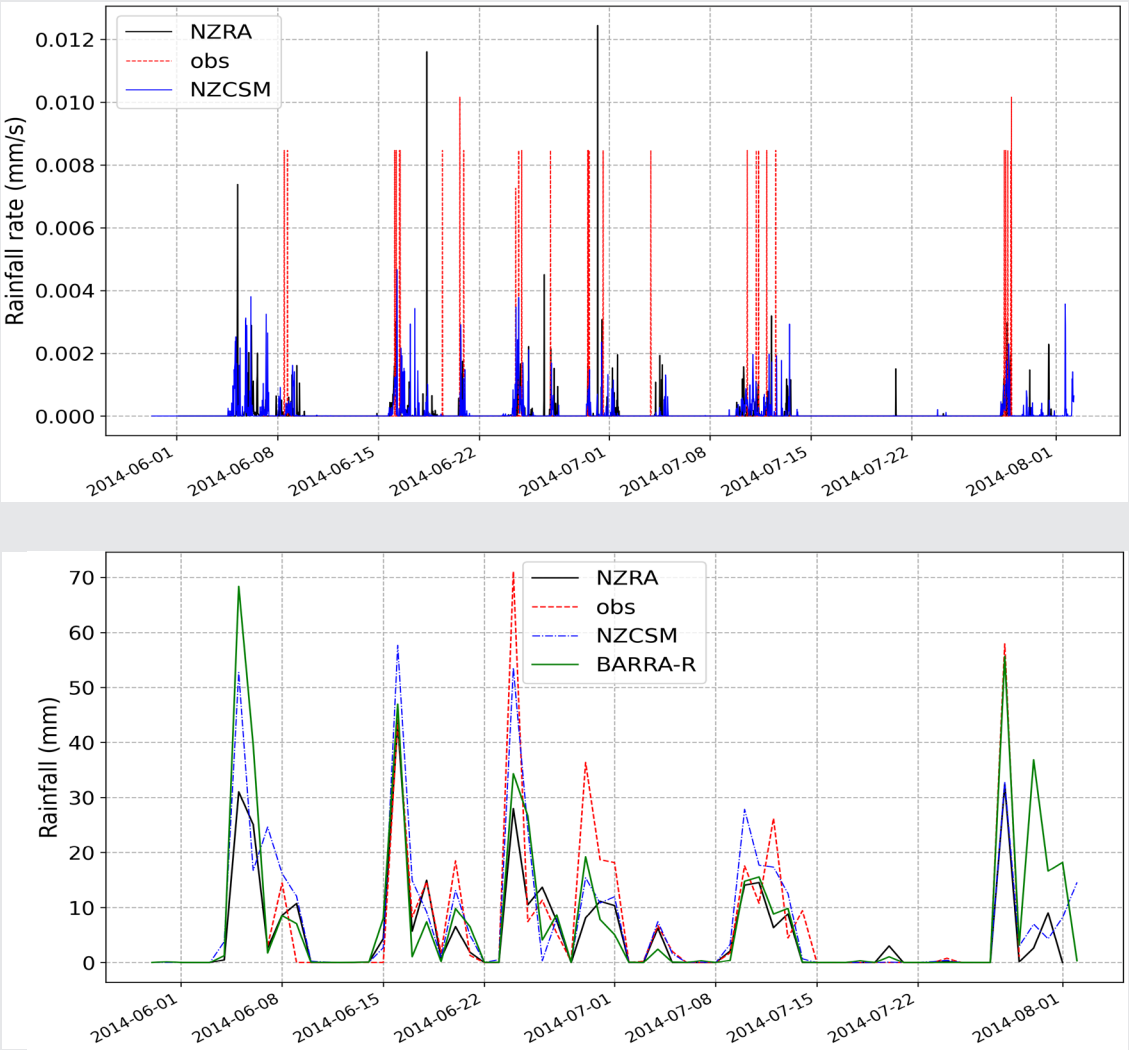

Figure 9: Comparison at Hokitika, New Zealand, during June-July 2014 of **(a)** Instantaneous rainfall rate timeseries at 30 minute intervals from point observations and closest NZRA and NZCSM grid points, and **(b)** daily accumulated precipitation, from point observations and closest NZRA, NZCSM and BARRA-R grid points.

in precipitation and frequency of high gust and mean wind speeds in the NZRA, NZCSM, BARRA-R and ERA datasets. Concentrating only on the non-ERA datasets first, the biases in the accumulated daily precipitation of the regional reanalyses are calculated using Eq. 1 with respect to the Augmented VCSN values for June-July 2014.

Due to the orographic induced rainfall over the Southern Alps, there is generally much more rainfall over the western side of the South Island than over other areas

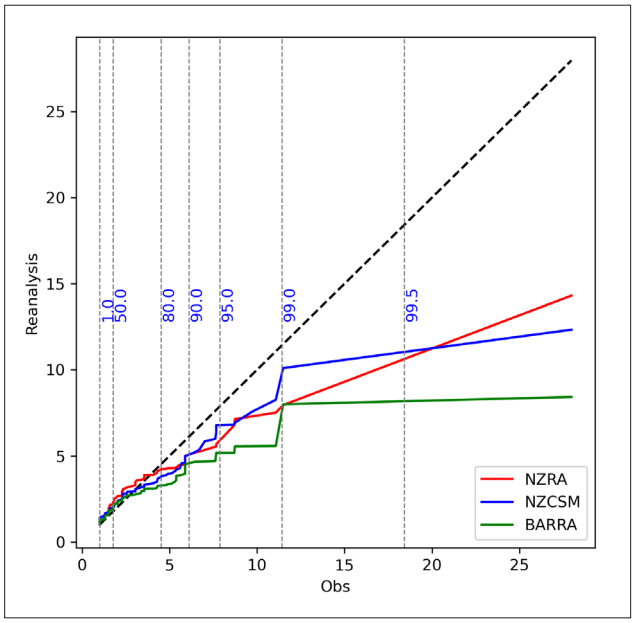

Figure 10: Comparisons of percentile values between observations at Hokitika and reanalyses for hourly accumulated precipitation greater than 1mm. The vertical dash lines indicate the corresponding percentiles of the observations.

al., 2019) and other reanalyses (Minola et al., 2020). Safaei Pirooz et al (2022) also showed that BARRA-R, unlike ERA5, does not capture the high gust wind speeds over the more southern mountains of the South Island. Figure 12 compares the frequency of gust wind speeds exceeding 25ms^{-1} in all the datasets considered in this study.

Similar to the analysis in Safaei Pirooz et al (2022), Figure 12 depicts that BARRA-R is unable to simulate strong wind speeds over the Southern Alps and other high peaks such as Mount Taranaki, and consequently shows lower occurrence of these events. All of the datasets show signs of similar high gust wind speed regions offshore, but NZRA and NZCSM deviate significantly over land from BARRA-R, ERA5 and ERA-Interim, particularly over high elevation regions, due to their higher spatial resolution being better able to resolve NZ's mountainous terrain. NZRA exhibits a higher frequency of strong winds compared to NZCSM over a larger area of mountainous terrain, particularly the central and southern most peaks of the South Island and Tararua, Ruahine and Central Plateau regions of the North

	North Island MAE (mm)	South Island MAE (mm)
NZRA	64.241	102.380
NZCSM	73.451	119.318
BARRA-R	78.269	116.785

Table 6: Mean absolute errors of total accumulated precipitation (during 30/05/2014 – 01/08/2014) between VCSN and NWP models.

of the country. One of the known issues of BARRA-R is that it overestimates precipitation over regions with high elevations (Su et al., 2019), as can also be seen along the west coast of the South Island in Figure 11b. In comparison, the NZRA shows smaller wet bias in precipitation in high-elevation regions compared with BARRA-R and NZCSM. Additionally, across the North Island (Figure 11a), NZRA also exhibits smaller biases, particularly over the west coast and southeast part of the North Island. NZCSM has a predominately wet bias over much of the North Island, with NZRA following BARRA-R in terms of spatial distribution of wet and dry biases over the North Island, but the magnitude of the bias is often smaller (Figure 11a). and BARRA-R have wet and dry biases over the most part of the island. A notable exception being over the Auckland region.

Positive and negative biases during light and strong wind events are another identified issue in BARRA-R (Su et

Island. The other reanalyses, BARRA-R, ERA5 and ERA-Interim, significantly underestimate strong winds and their frequency over land.

Similar performances can be seen in the frequency of relatively strong surface mean wind speeds in Figure 13. Here, frequency of surface mean wind speeds greater than 5ms^{-1} over New Zealand are plotted. More so than in Figure 12, a stark north-south split is exhibited in the BARRA-R, ERA5 and ERA-Interim datasets, all three indicating very little occurrence of >5ms^{-1} mean wind speeds over the South Island compared to NZRA and NZCSM. Comparing against VCSN data, Safaei Pirooz et al. (2022) showed previously that BARRA-R, ERA5 and ERA-Interim have large negative biases in mean surface wind speed over the South Island generally, so the higher frequency of >5ms^{-1} mean wind speeds over the South Island in NZRA represents a clear improvement over the other reanalysis datasets.

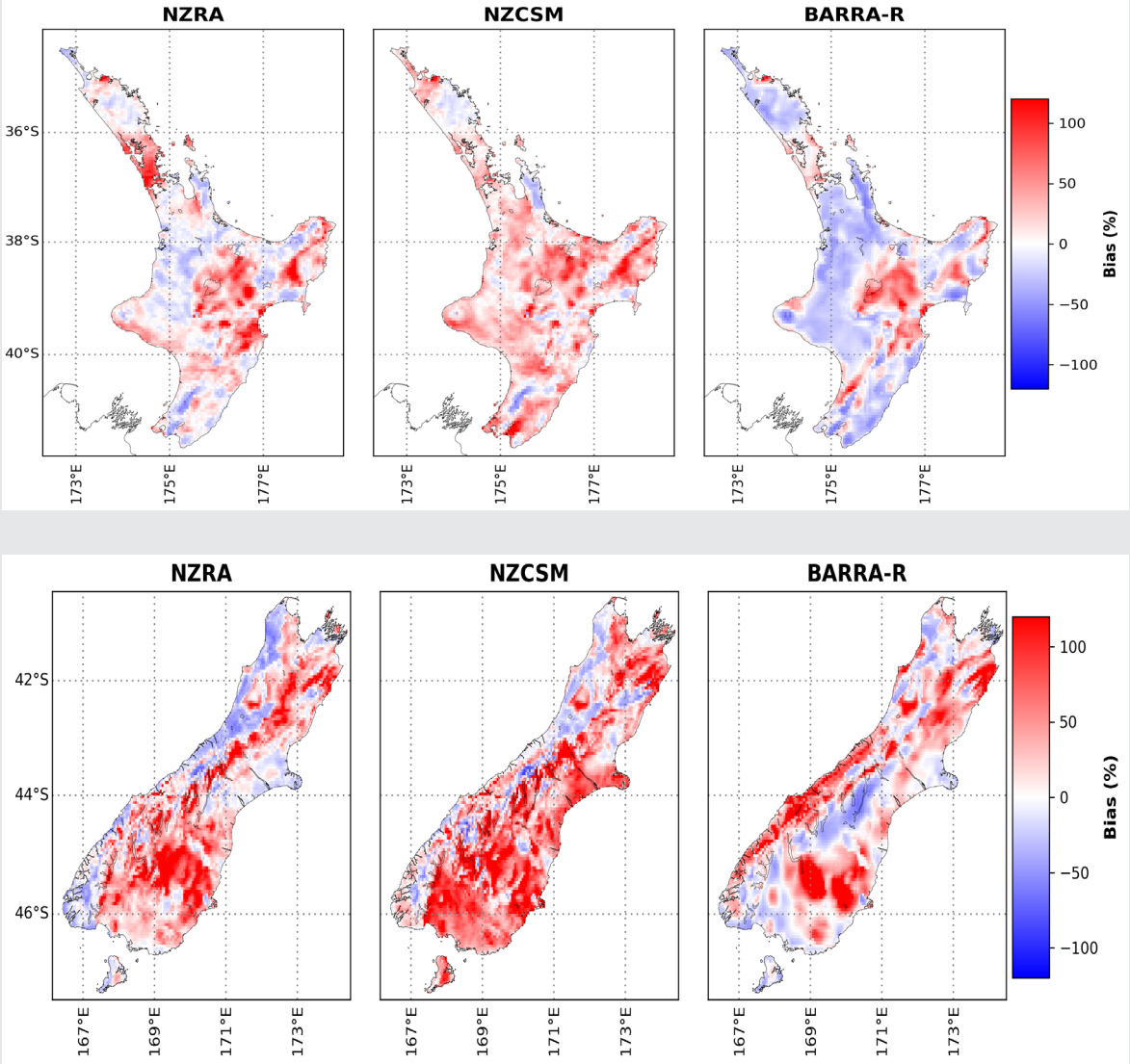

Figure 11: Mean bias percentages in daily accumulated precipitation during June-July 2014 from NZRA (left), NZCSM (middle) and BARRA-R (right) against the augmented VCSN across: (a) North Island, and (b) South Island.

4. CONCLUSION

This paper describes the development of the first high-resolution convective-permitting regional reanalysis model for New Zealand, called New Zealand Reanalysis (NZRA). NZRA, with a spatial horizontal grid spacing of 1.5km and 30 minute temporal resolution, is based on the UK Met Office Unified Model and is dynamically downscaled from the recently developed Bureau of Meteorology Atmospheric high-resolution Regional Reanalysis for Australia (BARRA-R) with approximately 12km horizontal resolution. BARRA-R provides both the initial and lateral boundary conditions to NZRA.

NZRA performance against independent observation data collected for the DEEPWAVE period (June – July 2014), has been evaluated to demonstrate its skill compared to existing global and regional reanalyses that cover New Zealand. It is shown that NZRA provides significantly better estimates of surface temperature for all percentiles and temperature ranges. In addition, NZRA surface wind speeds are closer to observations, particularly above the 90th percentile, compared with the other datasets. The biases in NZRA accumulated daily precipitation are generally smaller than NZCSM and BARRA-R over most of the North Island, and across the Canterbury region, West Coast and southern parts of the South Island. Standout areas where

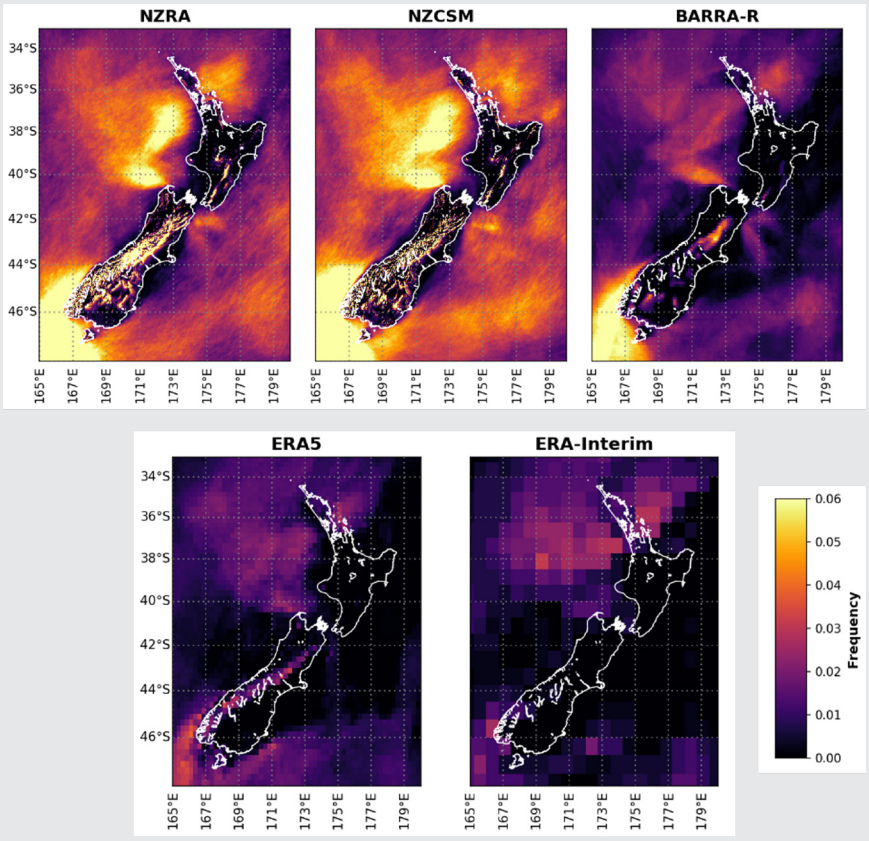

Figure 12: Frequency (ranging 0 to 1) of gust wind speeds greater than 25ms^{-1} over New Zealand for the period June – July 2014 from the different reanalyses and NZCSM. The native temporal resolution of each product (see Table 1) has been used in the calculation of frequencies.

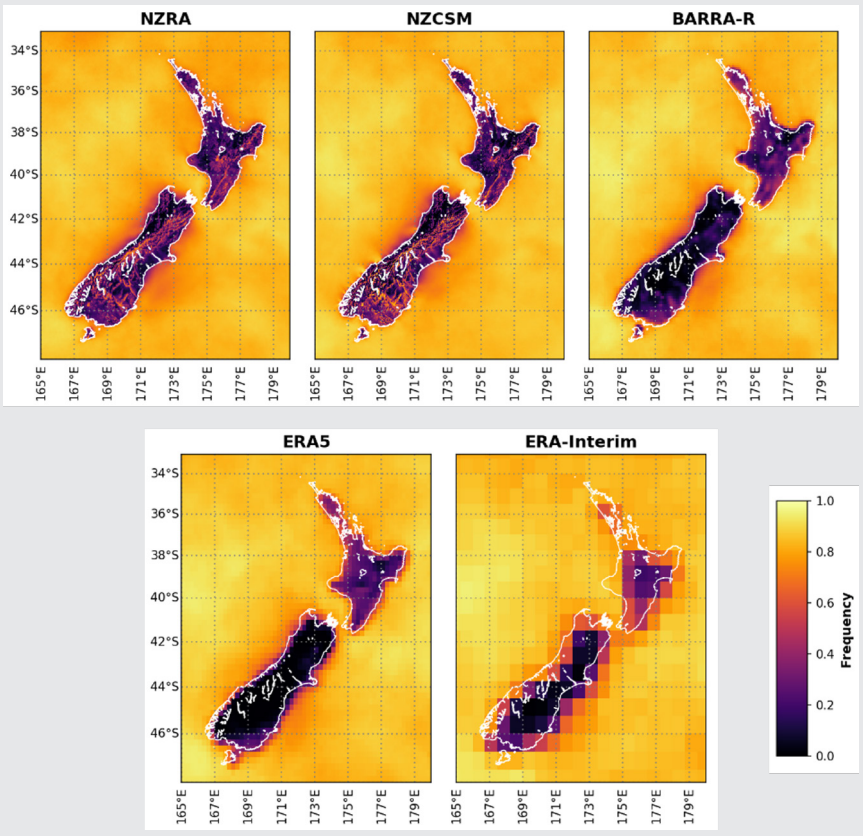

Figure 13: Frequency of surface mean wind speeds greater than 5ms^{-1} over New Zealand for the period June-July 2014 from the different reanalyses and NZCSM. The native temporal resolution of each product (see Table 1) has been used in the calculation of frequencies.

NZRA has larger biases than BARRA-R in particular are over the Auckland region (wetter) and southeastern parts of Fiordland (wetter). In addition, it appears that, for the trial period, NZRA provides an acceptable estimate of timing and intensity of rainfall rates. NZRA also outperforms its driving model in predicting strong winds over high elevation regions. Considering that the validation period was relatively short, a more comprehensive evaluation of NZRA will be conducted in future.

One of the limitations of the NZRA setup is the relatively short forecast length (9 hours) and short spin-up period (3 hours). The latter could lead to the model spin-up artefacts to still be present, especially convective clouds and rainfall as also elaborated by (Su et al., 2021). Nevertheless, NZRA outperforms its driving model and other global reanalyses in predicting precipitation, temperature and wind speed, particularly over mountainous and coastal regions.

NZRA will provide a deeper understanding of past climatology and extreme weather at local scales, particularly in places where long-term observations are not available. This knowledge can potentially contribute to several disciplines, including engineering design projects, meteorological and climatological studies, enhancing climate projection models, environmental studies, and risk and hazard assessments. Production runs of NZRA are currently underway at NIWA and will cover the 1990 – 2018 period.

ACKNOWLEDGMENTS

The authors wish to acknowledge the use of New Zealand eScience Infrastructure (NeSI) high performance computing facilities, consulting support and/or training services as part of this research. New Zealand's national facilities are provided by NeSI and funded jointly by NeSI's collaborator institutions and through the Ministry of Business, Innovation & Employment's Research Infrastructure programme. URL https://www.nesi.org.nz. We would also like to thank the Bureau of Meteorology, Australia, for providing the BARRA-R input data. We would also like to acknowledge NIWA's Strategic Science Investment Fund that supports this project.

REFERENCES

Acharya, S.C., Nathan, R., Wang, Q.J., Su, C.H., Eizenberg, N., 2019. An evaluation of daily precipitation from a regional atmospheric reanalysis over Australia. *Hydrol. Earth Syst. Sci*., 23, 3387-3403. DOI: https://10.5194/hess-23-3387-2019

Ashrit, R., Indira Rani, S., Kumar, S., Karunasagar, S., Arulalan, T., Francis, T., Routray, A., Laskar, S.I., Mahmood, S., Jermey, P., Maycock, A., Renshaw, R., George, J.P., Rajagopal, E.N., 2020. IMDAA Regional Reanalysis: Performance Evaluation During Indian Summer Monsoon Season. *Journal of Geophysical Research: Atmospheres,* 125, e2019JD030973. DOI: https://doi.org/10.1029/2019JD030973

Bannister, R.N., 2017. A review of operational methods of variational and ensemble-variational data assimilation. *Quarterly Journal of the Royal Meteorological Society*, 143, 607-633. DOI: https://doi.org/10.1002/qj.2982

Bush, M., Allen, T., Bain, C., Boutle, I., Edwards, J., Finnenkoetter, A., Franklin, C., Hanley, K., Lean, H., Lock, A., Manners, J., Mittermaier, M., Morcrette, C., North, R., Petch, J., Short, C., Vosper, S., Walters, D., Webster, S., Weeks, M., Wilkinson, J., Wood, N., Zerroukat, M., 2020. The first Met Office Unified Model–JULES Regional Atmosphere and Land configuration, RAL1. *Geosci. Model Dev*., 13, 1999-2029. DOI: https://10.5194/gmd-13-1999-2020

Carey-Smith, T., Andrews, P., 2016. Convective scale model verification – what can we do and what can we say?, Convective Scale Modelling Workshop, Park Royal Hotel, Singapore.

Clark, P., Roberts, N., Lean, H., Ballard, S.P., Charlton-Perez, C., 2016. Convection-permitting models: a step-change in rainfall forecasting. *Meteorological Applications*, 23, 165-181. DOI: https://doi.org/10.1002/met.1538

Davies, T., Cullen, M.J.P., Malcolm, A.J., Mawson, M.H., Staniforth, A., White, A.A., Wood, N., 2005. A new dynamical core of the Met Office's global and regional modelling of the atmosphere. *Quarterly Journal of the Royal Meteorological Society*, 131, 1759-1782. DOI: https://10.1256/qj.04.101

Dee, D.P., Uppala, S.M., Simmons, A.J., Berrisford, P., Poli, P., Kobayashi, S., Andrae, U., Balmaseda, M.A., Balsamo, G., Bauer, P., Bechtold, P., Beljaars, A.C.M., van de Berg, L., Bidlot, J., Bormann, N., Delsol, C., Dragani, R., Fuentes, M., Geer, A.J., Haimberger, L., Healy, S.B., Hersbach, H., Hólm, E.V., Isaksen, L., Kållberg, P., Köhler, M., Matricardi, M., McNally, A.P., Monge-Sanz, B., Morcrette, J.J., Park, B.K., Peubey, C., de Rosnay, P., Tavolato, C., Thépaut, J.N., Vitart, F., 2011. The ERA-Interim reanalysis: configuration and performance of the data assimilation system. *Quarterly Journal of the Royal Meteorological Society*, 137, 553-597. DOI: https://doi.org/10.1002/qj.828

Ehard, B., Achtert, P., Dörnbrack, A., Gisinger, S., Gumbel, J., Khaplanov, M., Rapp, M., Wagner, J., 2016. Combination of Lidar and Model Data for Studying Deep Gravity Wave Propagation. *Monthly Weather Review*, 144, 77-98. DOI: https://10.1175/mwr-d-14-00405.1

Frank, C.W., Pospichal, B., Wahl, S., Keller, J.D., Hense, A., Crewell, S., 2020. The added value of high resolution regional reanalyses for wind power applications. *Renewable Energy*, 148, 1094-1109. DOI: https://doi.org/10.1016/j.renene.2019.09.138

Fritts, D.C., Smith, R.B., Taylor, M.J., Doyle, J.D., Eckermann, S.D., Dörnbrack, A., Rapp, M., Williams, B.P., Pautet, P.-D., Bossert, K., Criddle, N.R., Reynolds, C.A., Reinecke, P.A., Uddstrom, M., Revell, M.J., Turner, R., Kaifler, B., Wagner, J.S., Mixa, T., Kruse, C.G., Nugent, A.D., Watson, C.D., Gisinger, S., Smith, S.M., Lieberman, R.S., Laughman, B., Moore, J.J., Brown, W.O., Haggerty, J.A., Rockwell, A., Stossmeister, G.J., Williams, S.F., Hernandez, G., Murphy, D.J., Klekociuk, A.R., Reid, I.M., Ma, J., 2016. The Deep Propagating Gravity Wave Experiment (DEEPWAVE): An Airborne and Ground-Based Exploration of Gravity Wave Propagation and Effects from Their Sources throughout the Lower and Middle Atmosphere. *Bulletin of the American Meteorological Society*, 97, 425-453. DOI: https://10.1175/bams-d-14-00269.1

Fuhrer, J., Beniston, M., Fischlin, A., Frei, C., Goyette, S., Jasper, K., Pfister, C., 2006. Climate Risks and Their Impact on Agriculture and Forests in Switzerland. *Climatic Change*, 79, 79-102. DOI: https://10.1007/s10584-006-9106-6

Gleixner, S., Demissie, T., Diro, G.T., 2020. Did ERA5 Improve Temperature and Precipitation Reanalysis over East Africa? *Atmosphere*, 11, 996.

GLOBE Task Team, 1999. The Global Land One-kilometre Base Elevation (GLOBE) Digital Elevation Model, Version 1.0, in: Hastings, D.A., Dunbar, P.K., Elphingstone, G.M., Bootz, M., Murakami, H., Maruyama, H., Masaharu, H., Holland, P., Payne, J., Bryant, N.A., Logan, T.L., Muller, J.P., Schreier, G., John, S.M. (Eds.). National Oceanic and Atmospheric Administration, National Geophysical Data Center, 325 Broadway, Boulder, Colorado 80305-3328, U.S.A.

Hanley, K., Whitall, M., Stirling, A., Clark, P., 2019. Modifications to the representation of subgrid mixing in kilometre-scale versions of the Unified Model. *Quarterly Journal of the Royal Meteorological Society*, 145, 3361-3375. DOI: https://doi.org/10.1002/qj.3624

Hartley, A.J., MacBean, N., Georgievski, G., Bontemps, S., 2017. Uncertainty in plant functional type distributions and its impact on land surface models. *Remote Sensing of Environment*, 203, 71-89. DOI: https://doi.org/10.1016/j.rse.2017.07.037

Hersbach, H., et al., 2020. The ERA5 global reanalysis. *Quarterly Journal of the Royal Meteorological Society*, 146, 1999-2049. DOI: https://doi.org/10.1002/qj.3803

Hu, G., Franzke, C.L.E., 2020. Evaluation of Daily Precipitation Extremes in Reanalysis and Gridded Observation-Based Data Sets Over Germany. *Geophysical Research Letters*, 47, e2020GL089624. DOI: https://doi.org/10.1029/2020GL089624

Keller, J.D., Wahl, S., 2021. Representation of Climate in Reanalyses: An Intercomparison for Europe and North America. *Journal of Climate*, 34, 1667-1684. DOI: https://10.1175/jcli-d-20-0609.1

Komurcu, M., Emanuel, K.A., Huber, M., Acosta, R.P., 2018. High-Resolution Climate Projections for the Northeastern United States Using Dynamical Downscaling at Convection-Permitting Scales. *Earth and Space Science*, 5, 801-826. DOI: https://doi.org/10.1029/2018EA000426

Leeper, R.D., Bell, J.E., Vines, C., Palecki, M., 2017. An Evaluation of the North American Regional

Reanalysis Simulated Soil Moisture Conditions during the 2011–13 Drought Period. *Journal of Hydrometeorology*, 18, 515-527. DOI: https://10.1175/jhm-d-16-0132.1

Lu, J., Carbone, G.J., Gao, P., 2019. Mapping the agricultural drought based on the long-term AVHRR NDVI and North American Regional Reanalysis (NARR) in the United States, 1981–2013. *Applied Geography*, 104, 10-20. DOI: https://doi.org/10.1016/j.apgeog.2019.01.005

Lu, Y., Fang, J., Pan, Y., Wang, S., Zhou, P., Yang, Y., Shao, M., Tang, J., 2021. Evaluation of 12-Years Chinese Regional Reanalysis (1998–2009): Comparison of Dynamical Downscaling Methods With/Without Local Data. *Journal of Geophysical Research: Atmospheres,* 126, e2020JD034259. DOI: https://doi.org/10.1029/2020JD034259

Mesinger, F., DiMego, G., Kalnay, E., Mitchell, K., Shafran, P.C., Ebisuzaki, W., Jović, D., Woollen, J., Rogers, E., Berbery, E.H., Ek, M.B., Fan, Y., Grumbine, R., Higgins, W., Li, H., Lin, Y., Manikin, G., Parrish, D., Shi, W., 2006. North American Regional Reanalysis. *Bulletin of the American Meteorological Society*, 87, 343-360. DOI: https://10.1175/bams-87-3-343

Miller, N.L., Bashford, K.E., Strem, E., 2003. Potential Impacts of Climate Change On California Hydrology. *Journal of the American Water Resources Association* (JAWRA), 39, 771-784. DOI: https://doi.org/10.1111/j.1752-1688.2003.tb04404.x

Minola, L., Zhang, F., Azorin-Molina, C., Pirooz, A.A.S., Flay, R.G.J., Hersbach, H., Chen, D., 2020. Near-surface mean and gust wind speeds in ERA5 across Sweden: towards an improved gust parametrization. *Climate Dynamics*, 55, 887-907. DOI: https://doi.org/10.1007/s00382-020-05302-6

Rose, S., Apt, J., 2016. Quantifying sources of uncertainty in reanalysis derived wind speed. *Renewable Energy*, 94, 157-165. DOI: https://doi.org/10.1016/j.renene.2016.03.028

Safaei Pirooz, A.A., Moore, S., Carey-Smith, T., Turner, R., Su, C.H., 2022. Evaluation of global and regional reanalyses performance over New Zealand. *Weather & Climate*, 41, 16-35.

Steinheuer, J., Friederichs, P., 2020. Vertical profiles of wind gust statistics from a regional reanalysis using multivariate extreme value theory. *Nonlin. Processes Geophys.*, 27, 239-252. DOI: https://10.5194/npg-27-239-2020

Steinke, S.W., Sabrina; Crewell, Susanne, 2019. Benefit of high resolution COSMO reanalysis: The diurnal cycle of column-integrated water vapor over Germany. *Meteorologische Zeitschrift*, 28, 165-177. DOI: https://10.1127/metz/2019/0936

Su, C.H., Eizenberg, N., Jakob, D., Fox-Hughes, P., Steinle, P., White, C.J., Franklin, C., 2021. BARRA v1.0: kilometre-scale downscaling of an Australian regional atmospheric reanalysis over four midlatitude domains. *Geoscientific Model Development*, 14, 4357-4378. DOI: https://10.5194/gmd-14-4357-2021

Su, C.H., Eizenberg, N., Steinle, P., Jakob, D., Fox-Hughes, P., White, C.J., Rennie, S., Franklin, C., Dharssi, I., Zhu, H., 2019. BARRA v1.0: the Bureau of Meteorology Atmospheric high-resolution Regional Reanalysis for Australia. *Geoscientific Model Development*, 12, 2049-2068. DOI: https://10.5194/gmd-12-2049-2019

Tait, A., Henderson, R., Turner, R., Zheng, X., 2006. Thin plate smoothing spline interpolation of daily rainfall for New Zealand using a climatological rainfall surface. *International Journal of Climatology*, 26, 2097-2115. DOI: https://10.1002/joc.1350

Tait, A., Sturman, J., Clark, M., 2012. An assessment of the accuracy of interpolated daily rainfall for New Zealand. *Journal of Hydrology* (NZ), 51, 25-44.

Tait, A., Turner, R., 2005. Generating Multiyear Gridded Daily Rainfall over New Zealand. *Journal of Applied Meteorology*, 44, 1315-1323.

Taszarek, M., Allen, J.T., Púčik, T., Hoogewind, K.A., Brooks, H.E., 2020. Severe Convective Storms across Europe and the United States. Part II: ERA5 Environments Associated with Lightning, Large Hail, Severe Wind, and Tornadoes. *Journal of Climate*, 33, 10263-10286. DOI: https://10.1175/jcli-d-20-0346.1

Tetzner, D., Thomas, E., Allen, C., 2019. A Validation of ERA5 Reanalysis Data in the Southern Antarctic Peninsula—Ellsworth Land Region, and Its Implications for Ice Core Studies. *Geosciences*, 9, 289. DOI: https://10.3390/geosciences9070289

Turner, R., Moore, S., 2017. An analysis of three years of Convective Scale Numerical Model diagnosed gusts over New Zealand, 9th Asia-Pacific Conference on Wind Engineering, Auckland, New Zealand.

Witschas, B., Rahm, S., Dörnbrack, A., Wagner, J., Rapp, M., 2017. Airborne Wind Lidar Measurements of Vertical and Horizontal Winds for the Investigation of Orographically Induced Gravity Waves. *Journal of Atmospheric and Oceanic Technology*, 34, 1371-1386. DOI: https://10.1175/jtech-d-17-0021.1

Wood, N., Staniforth, A., White, A., Allen, T., Diamantakis, M., Gross, M., Melvin, T., Smith, C., Vosper, S., Zerroukat, M., Thuburn, J., 2014. An inherently mass-conserving semi-implicit semi-Lagrangian discretization of the deep-atmosphere global non-hydrostatic equations. *Quarterly Journal of the Royal Meteorological Society*, 140, 1505-1520. DOI: https://doi.org/10.1002/qj.2235

Yang, Y., Moore, S., Uddstrom, M., Turner, R., Carey-Smith, T., 2017. Model moist bias in the middle and upper troposphere during DEEPWAVE. *Atmospheric Science Letters*, 18, 161-167. DOI: https://doi.org/10.1002/asl.738

Yoshimura, K., Kanamitsu, M., 2008. Dynamical Global Downscaling of Global Reanalysis. *Monthly Weather Review*, 136, 2983-2998. DOI: https://10.1175/2008mwr2281.1

Zhang, H., Cao, Y., Zhang, Y., Terzija, V., 2018. Quantitative synergy assessment of regional wind-solar energy resources based on MERRA reanalysis data. *Applied Energy*, 216, 172-182. DOI: https://doi.org/10.1016/j.apenergy.2018.02.094